

Original Article

Efficacy of a newly designed helical-shaped 3D-printed titanium cage for cervical vertebral defect healing in rabbits

Mosharraf Hossain¹, Soobin Im^{1,2}, Je Hoon Jeong¹, Tamima Sultana¹, Jung Hoon Kang¹, Byong-Taek Lee^{2,3}

¹Department of Neurosurgery, College of Medicine, Soonchunhyang University, Bucheon Hospital, Bucheon, South Korea; ²Institute of Tissue Regeneration, Soonchunhyang University, Cheonan, South Korea; ³Department of Regenerative Medicine, Soonchunhyang University, Cheonan, South Korea

Received August 23, 2022; Accepted December 13, 2022; Epub January 15, 2023; Published January 30, 2023

Abstract: Three-dimensional (3D) printed titanium (Ti-6Al-4V alloy) cages are widely used for spinal fusion applications. However, the structural design and shape of the cages are a major determinant of the optimal clinical outcome. In this study, we constructed a newly designed 3D-printed helical-shaped titanium cage (HTC) with a flexible body, and compared its healing and fusion efficacy in cervical vertebral defects after corpectomy in rabbits to that of a 3D-printed traditional titanium cage (TTC). We performed radiological examinations 1 and 16 weeks after TTC and HTC implantation. We assessed bone ingrowth in TTC and HTC using micro-computed tomography (micro-CT) and histological staining of tissue sections at 16 weeks. The radiographic data showed that the HTC-implanted group had better restoration of vertebral height than the TTC group, indicating a lower risk of cage subsidence. The micro-CT and histological observations showed that HTC promoted bone regeneration and osseointegration more effectively than TTC. Histomorphometry further revealed significant new bone formation in the HTC group compared to the TTC group. These findings demonstrate that HTC has better healing and bone fusion effects than TTC in cervical vertebral defects in rabbits, indicating its potential clinical value.

Keywords: Cervical vertebral defects, 3D-printing, titanium cage, osseointegration, bone ingrowth

Introduction

Anterior cervical corpectomy and fusion (ACCF) is an effective procedure for the treatment of degenerative cervical spine pathologies, especially cervical spondylotic myelopathy (CSM) and ossified posterior longitudinal ligaments (OPLL) [1, 2]. ACCF involves decompression of the spinal cord and reconstruction of the damaged vertebrae [3]. After the corpectomy, the vertebral defects are commonly reconstructed with autogenous bone grafts and allografts [2, 4, 5]. However, use of these bone grafts is limited due to donor-site morbidity and other serious complications, such as pain, infection, and hematomas. To fix these issues, cervical reconstruction with a titanium mesh cage (TMC) is effectively performed after corpectomy due to its clinical efficacy, biocompatibility, high fusion rate, and ability to restore spinal alignment [6-9].

However, TMC subsidence is frequently observed during the early postoperative period due to its higher elastic modulus and stress-shielding effect [10, 11]. Subsidence is defined as the loss of vertebral height between adjacent vertebral endplates after ACCF, and is a common mechanical complication affecting up to 93.3% of cases [12]. In addition, many studies have reported problems with TMC design and shape, which might affect cage subsidence and the bone fusion rate. The traditional TMC has a limited area of contact with the endplate, resulting in implant failure after implantation [13]. Various methods, such as use of an end cap, anatomical cage, dome-shaped cage, and fornix-shaped cage, have been proposed to address these problems [11, 13, 14].

Recently, three-dimensional (3D) printing has been used to fabricate titanium (Ti) implants for bone tissue engineering and spinal fusion appli-

3D-printed titanium cage for cervical vertebral defect repair

cations. 3D printing can introduce various designs and shapes of Ti implants with low elastic moduli via computer-aided design (CAD). Therefore, 3D-printed Ti implants with an appropriate shape can be produced for spinal fusion surgery with a lower risk of cage subsidence, uniform surface, and porous structure [15-17]. Moreover, 3D printing can be used to fabricate implants with a rough surface to enhance osseointegration at the implantation site [18-21].

In the present study, we fabricated a novel 3D-printed helical-shaped titanium cage (HTC) with a flexible body, and compared it with a 3D-printed traditional titanium cage (TTC) in terms of healing and bone fusion of cervical vertebral defects after corpectomy in a rabbit model. We also evaluated the height of the operated vertebral segment after implantation to investigate cage subsidence risk.

Materials and methods

Implant material and fabrication technology

Powdered Ti-6Al-4V ELI alloy (ASTM standard, grade 23) was used to fabricate the 3D-printed samples in this study. The implants were initially designed using CAD and then a 3D-printer (M280; EOS, Krailling, Germany) was used to fabricate the final scaffold via direct metal laser sintering [22, 23]. Each cage has two points for screw insertion.

Morphology and mechanical properties

A digital microscope was used to observe the shape and design of the samples in various positions. The surface morphology of the samples was investigated by scanning electron microscopy (SEM) (635F; JEOL, Tokyo, Japan). Briefly, the sample was placed in the SEM holder and sputter-coated with platinum (Cresington 108 Auto; JEOL) before SEM scanning. SEM images were taken at an acceleration voltage of 5 kV.

Mechanical testing of the TTC and HTC was performed using a universal testing machine (UTM; R & B, Seoul, South Korea). Three samples were used for each group. Compression was conducted at a rate of 0.5 mm/min during testing, and the load-displacement curves of the cages were obtained.

In vivo study

Animal models and ethics: Fourteen male New Zealand white (NZW) rabbits were purchased and raised in individual stainless steel cages for 7 days (as an acclimatization period) before surgery. Standard food and water were provided ad libitum throughout the study period. The animals were divided into two groups (both n=7), implanted with the TTC or HTC. The animal experiments were performed using a protocol approved by the Animal Ethics Committee of Soonchunhyang University Bucheon Hospital (approval number: SCABCA 2019-09; approval date: July 2019).

Surgical procedure: The animals were anesthetized with 5% isoflurane and a vaporizer mask was attached to maintain anesthesia and oxygen supply. The animals underwent surgery on an operating table in the supine position, with the neck extended but slightly flexed from the straight position to relieve the airway and allow placement of the vaporizer mask. A flexed neck position was important to maintain the airway and reduce respiratory distress during the cervical corpectomy surgery. After shaving the hair on the anterior part of the neck, the area was disinfected with 70% alcohol followed by 10% povidone-iodine solution, to prevent infection in the surgical area. The entire procedure was performed under a surgical microscope. We used a standard right anterior approach to expose the cervical spine through a 3-4 cm vertical incision for single-level corpectomy [24]. Briefly, the skin and platysma were incised vertically (**Figure 3A**) to expose the vertebral bodies and discs (**Figure 3B**). Depending on the size of the 3D-printed cage, an electric drill was used to prepare the corpectomy defects (**Figure 3C**). However, no attempt was made to excise the posterior longitudinal ligament or expose the spinal canal. The cage was implanted in the defect (**Figure 3D**) and immobilized with two screws (**Figure 3E** and **3F**). The incision site was cleaned with saline and sutured in a layer-by-layer manner.

Postoperative management and extraction of cervical spine

Analgesics and antibiotics were injected for 3 consecutive days to relieve pain and prevent postoperative infection, respectively. After 16

3D-printed titanium cage for cervical vertebral defect repair

weeks, the animals were euthanized and the cervical spine was extracted, followed by fixation in 10% neutral buffered formalin for further analyses.

Radiography and micro-computed tomography (Micro-CT) evaluation: Anteroposterior and lateral radiographs of the animals were obtained 1 and 16 weeks after the surgery. Cage dislocation, segment height of the operated vertebrae, and instrument stability were compared between 1 and 16 weeks using radiographs.

Micro-CT of the implanted cages was performed using a SkyScan Desktop Micro-CT 1172 (Bruker, Billerica, MA, USA), with a source voltage of 60 kV and current of 167 mA. The data were reconstructed with NRecon software and analyzed with CTAn software to calculate the bone volume/tissue volume (BV/TV) ratio in the implanted cages.

Histological and histomorphometric analysis: After nondestructive micro-CT analysis, the specimens were dehydrated through an alcohol series (70-100%) for histological evaluation. The specimens were immersed in Technovit 7200 solution (Kulzer, Hanau, Germany) for 7 days. The samples were embedded in methyl-methacrylate resin (Sigma-Aldrich) and cut into sections about 40 μ m thick. The samples were stained with hematoxylin and eosin (H & E) and Goldner's trichrome to evaluate new bone formation in the cages and osseointegration with the host bone. The slides were mounted, and images were acquired with a fluorescence microscope. For histomorphometry, the stained tissue sections were analyzed by Image-Pro Plus software to calculate new bone formation.

Statistical analysis

All tests were conducted at least in triplicate. All data are expressed as the mean \pm standard deviation (SD). Group differences in radiological data were calculated using Student's t-test. The micro-CT and histomorphometry measurements were analyzed statistically using one-way analysis of variance (ANOVA) followed by the *post hoc* Tukey's test. The results were considered statistically significant when $P < 0.05$.

Results

Implant morphology and compressive strength

Digital microscopy was used to inspect the gross structure and shape of the TTC and HTC, as shown in **Figure 1**. Top and rear views of TTC and HTC revealed that TTC was a simply designed cage with a larger gap (1 mm) between the horizontal layer and HTC had a helical shape in the body. Digital microscopy of the TTC (**Figure 1E**) showed an empty inner cavity, whereas the HTC (**Figure 1F**) had an hourglass-shaped inner cavity.

SEM images of the TTC and HTC are shown in **Figure 2A** and **2B**, respectively, where higher-magnification images revealed that both samples had a rough surface. HTC showed a more uniform surface structure (**Figure 2B**). The load-displacement indicated that TTC had comparatively higher compressive strength than HTC (**Figure 2C**).

In vivo performance

One animal died during surgery due to overexposure to anesthesia and excessive bleeding. We replaced it with a new animal from the same group. There were no significant differences in operating time or bleeding amount between the two groups. The peripheral oxygen saturation (SpO₂) level was excellent during the operation in both groups. No abnormalities were detected in any animals after implantation.

Radiological outcomes

Only one cage dislocation/migration was detected in a TTC-implanted group at the final follow-up x-ray examination (16 weeks). Radiographs confirmed that the TTC and HTC integrated well and were stable in the defect site (**Figure 4A**). No infection or inflammation of the surgical site was observed. The average segment height of the TTC was 23.3 ± 2.1 mm 1 week after implantation surgery and 21.6 ± 1.8 mm at 16 weeks (**Table 1**). The average segmental heights of the HTC at 1 and 16 weeks after the operation were 22.8 ± 1.4 and 21.9 ± 1.1 mm, respectively. The mean reductions of segmental height in the TTC and HTC groups were 1.8 ± 0.4 and 0.91 ± 0.3 mm, respectively (**Table 1**). As shown in **Figure 4B**, the TTC group

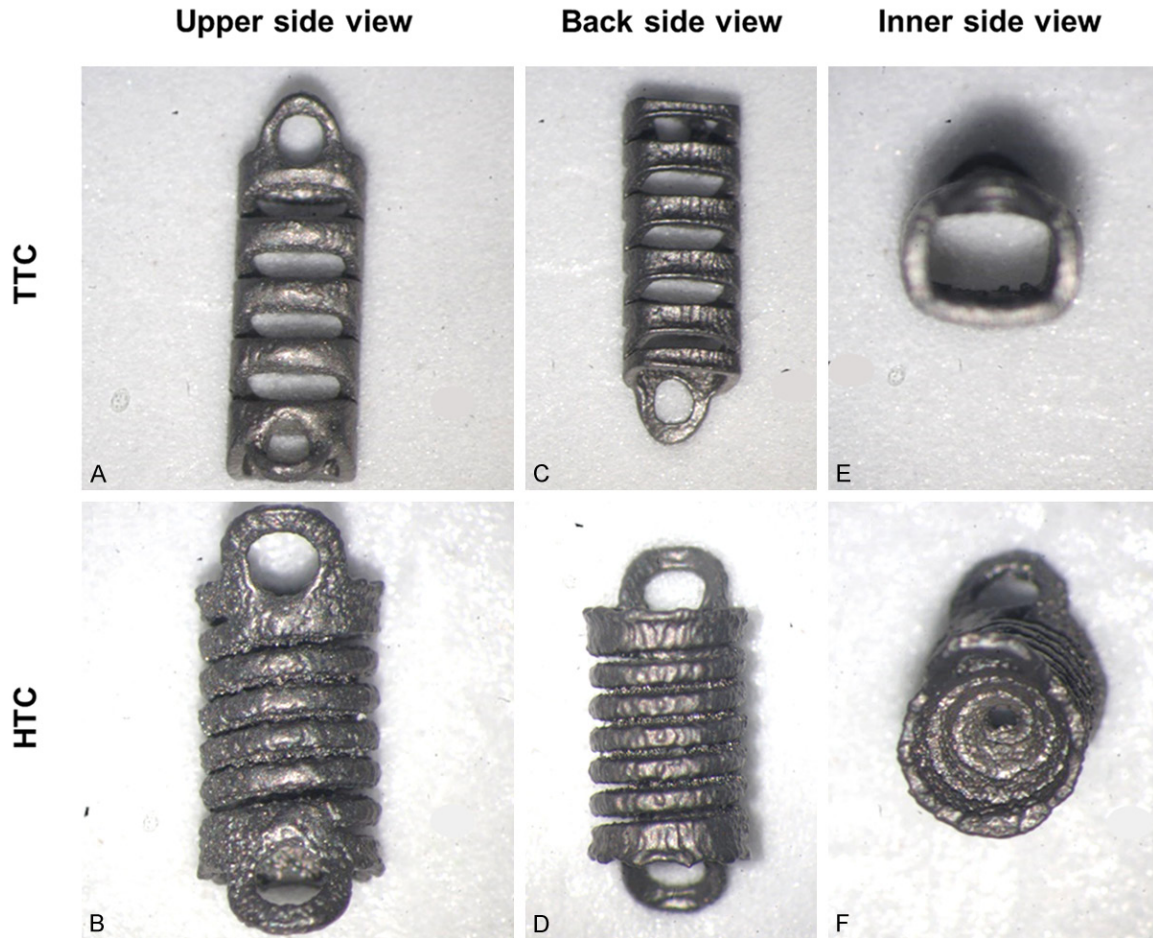


Figure 1. Digital photographs of a traditional titanium cage (TTC) and helical-shaped titanium cage (HTC) showing their gross morphology and design. Top and rear views showed that TTC (A, C) had a conventional structure with a larger gap between horizontal layers, while HTC (B, D) had a helical shape. Internal views of the TTC (E) and HTC (F) showed that TTC had an inner cavity, whereas HTC had a more complex structure.

showed a significant loss of vertebral segment height compared to the HTC group.

Micro-CT analysis

Micro-CT scanning indicated that the cages were well integrated and stable between the material and host bone, as shown by two-dimensional (2D) and 3D micro-CT images, respectively (**Figure 5B** and **5C**). No halo formation was observed around the inserted screws. The BV/TV ratio was significantly higher in the HTC than TTC group (25.67 ± 1.78 vs. 17.65 ± 1.67 , respectively, $P < 0.01$) (**Figure 5A**).

Histological observation and histomorphometric analysis

The TTC and HTC were investigated histologically 16 weeks after implantation in rabbit cervical vertebral defects. H & E and Goldner's tri-

chrome staining revealed no inflammatory cell infiltration in either implant. HTC showed better contact with the bone than TTC. Histological sections also showed more new bone formation with HTC than TTC around the implanted area at 16 weeks after implantation (**Figures 6** and **7**). The new bone extended into the inner side of the HTC, indicating greater bone regeneration capacity of HTC than TTC. Furthermore, more mineralized bone was observed in the HTC than TTC group (**Figure 7**). In addition, histomorphometric analysis revealed that HTC was associated with significantly more new bone formation than TTC, as shown in **Figure 8** ($P < 0.05$).

Discussion

Implant design and shape play vital roles in improving osseointegration and osteogenesis

3D-printed titanium cage for cervical vertebral defect repair

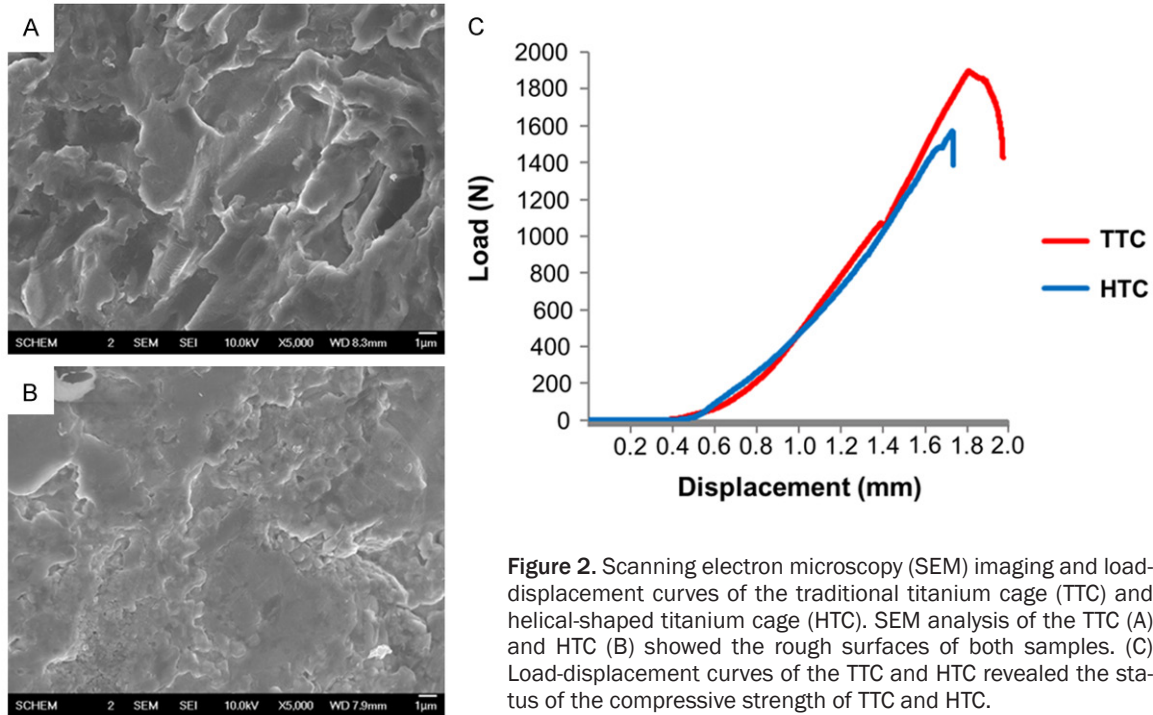


Figure 2. Scanning electron microscopy (SEM) imaging and load-displacement curves of the traditional titanium cage (TTC) and helical-shaped titanium cage (HTC). SEM analysis of the TTC (A) and HTC (B) showed the rough surfaces of both samples. (C) Load-displacement curves of the TTC and HTC revealed the status of the compressive strength of TTC and HTC.

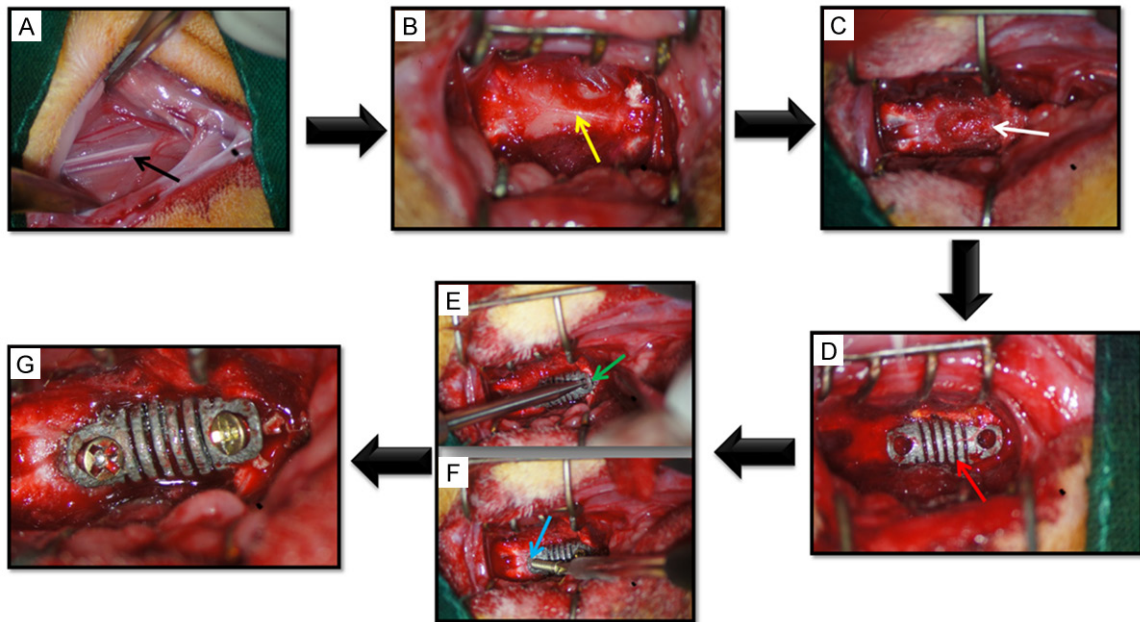


Figure 3. Implantation procedure. A. Skin incision and dissection of the muscles; the black arrow indicates the carotid artery. B. The spine and vertebral body (yellow arrow) were exposed by careful dissection. C. A defect (white arrow) was made in the C3/C4 vertebral body with an electric drill. D. The titanium cage was implanted in the defect indicated by the red arrow. E. Two holes were made with a drill to attach the screws (green arrow). F. The screws were then attached at the point shown by the blue arrow. G. Final view of the implanted cage.

at the implantation site, and therefore significantly affecting bone defect reconstruction and remodeling [25-27]. Bone remodeling and

new bone formation are also associated with load-bearing capacity according to Wolff's law [28]. Ti implants with a conventional shape and

3D-printed titanium cage for cervical vertebral defect repair

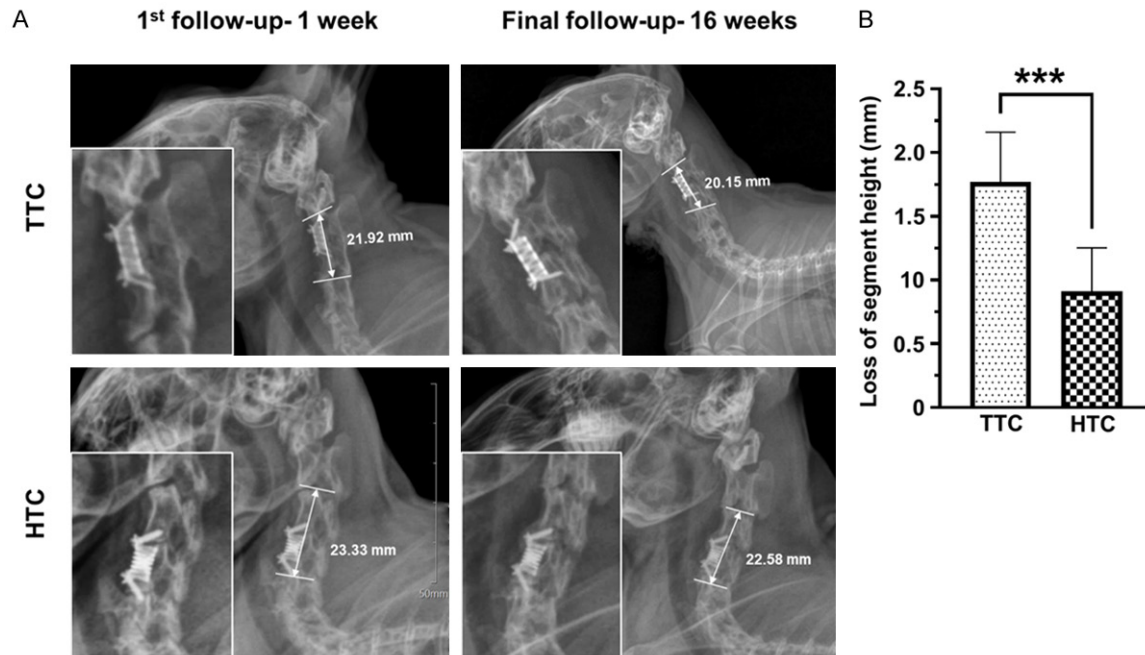


Figure 4. Radiographic analysis. A. Radiographs and vertebral segment height of the traditional titanium cage (TTC) and helical-shaped titanium cage (HTC)-implanted rabbits 1 and 16 weeks after surgery; the images showed the proper implantation and stabilization of the cages in the defect. B. Comparison of the loss of segment height after implantation with the TTC and HTC; similar lateral radiographs were used to compare the segment height between 1 and 16 weeks after implantation. The segment height was significantly reduced in the TTC compared to the HTC, so the TTC was associated with a significantly greater risk of cage subsidence during the postoperative period. All data are expressed as the mean \pm standard deviation (SD). *** $P < 0.001$.

Table 1. Radiological outcomes

| Parameters | TTC group | HTC group | P-value |
|---|----------------|----------------|---------|
| Mean segmental height after the operation, mm | 23.3 \pm 2.1 | 22.8 \pm 1.4 | 0.4595 |
| Mean segmental height after the final follow-up, mm | 21.6 \pm 1.8 | 21.9 \pm 1.1 | 0.6025 |
| Mean reduction in height (subsidence), mm | 1.8 \pm 0.4 | 0.91 \pm 0.3 | 0.0001 |
| Cage migration | 1 | 0 | |
| Screw pull-out | 1 | 0 | |
| Screw loosening | 0 | 1 | |
| Screw breakage | 0 | 0 | |

Values are number or mean \pm standard deviation (SD). TTC, traditional titanium cage; HTC, helical-shaped titanium cage.

solid design have a poor bone regeneration effect [29]. To resolve this issue and enhance osteogenesis, a number of porous implants with greater biocompatibility (which facilitates bone fusion) have been designed and fabricated using 3D printing [30]. Furthermore, the stress-shielding effect might also be prevented by modifying the implant's design and porous structure to reduce the elastic modulus closer to that of the host bone [19]. In this study, the HTC with a porous helical-shaped structure was investigated for its ability to promote cervical vertebral defect healing relative to the TTC.

Surface roughness is a crucial parameter that enhances the biomedical performance of Ti implants by promoting bone cell differentiation both *in vitro* and *in vivo* [31-33]. Rough surfaces were generated by 3D printing in the TTC and HTC in this study, as revealed by SEM (Figure 2A and 2B), and resulted in a favorable interaction between the implant and host tissue. In addition, variation in the shape and porous structure of the Ti implants provided different biocompatibility results *in vitro* and *in vivo* [34, 35]. However, there has been no previous report of Ti cage implantation in a cervical

3D-printed titanium cage for cervical vertebral defect repair

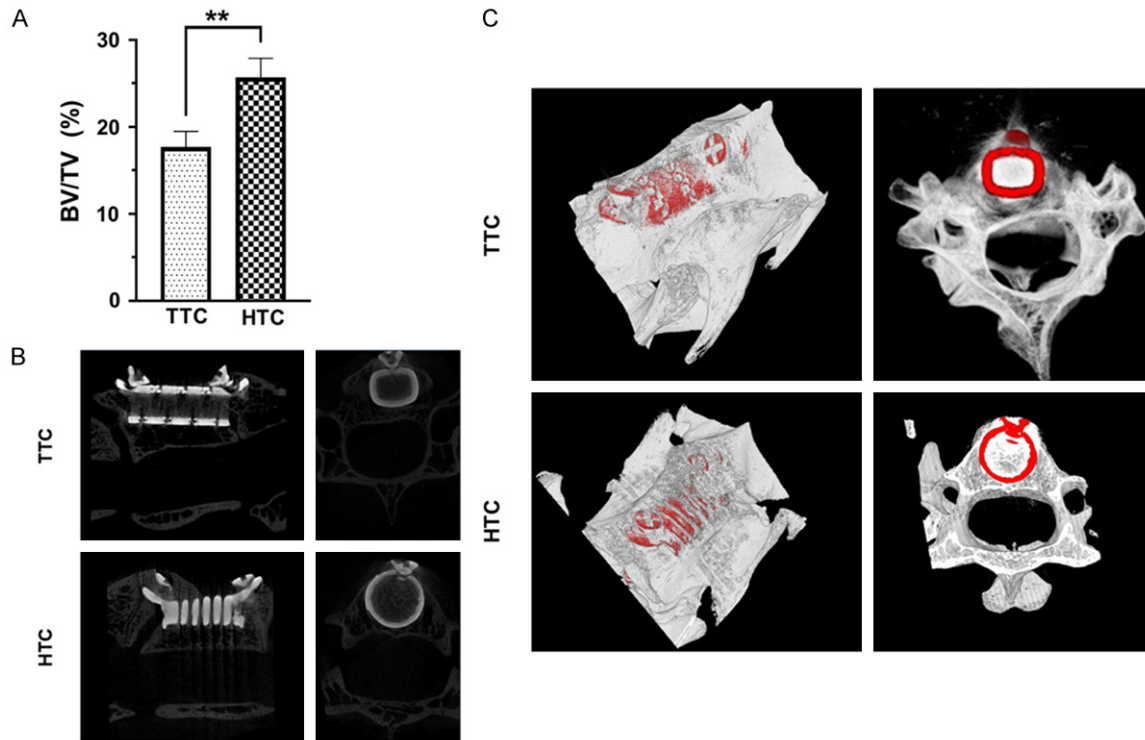
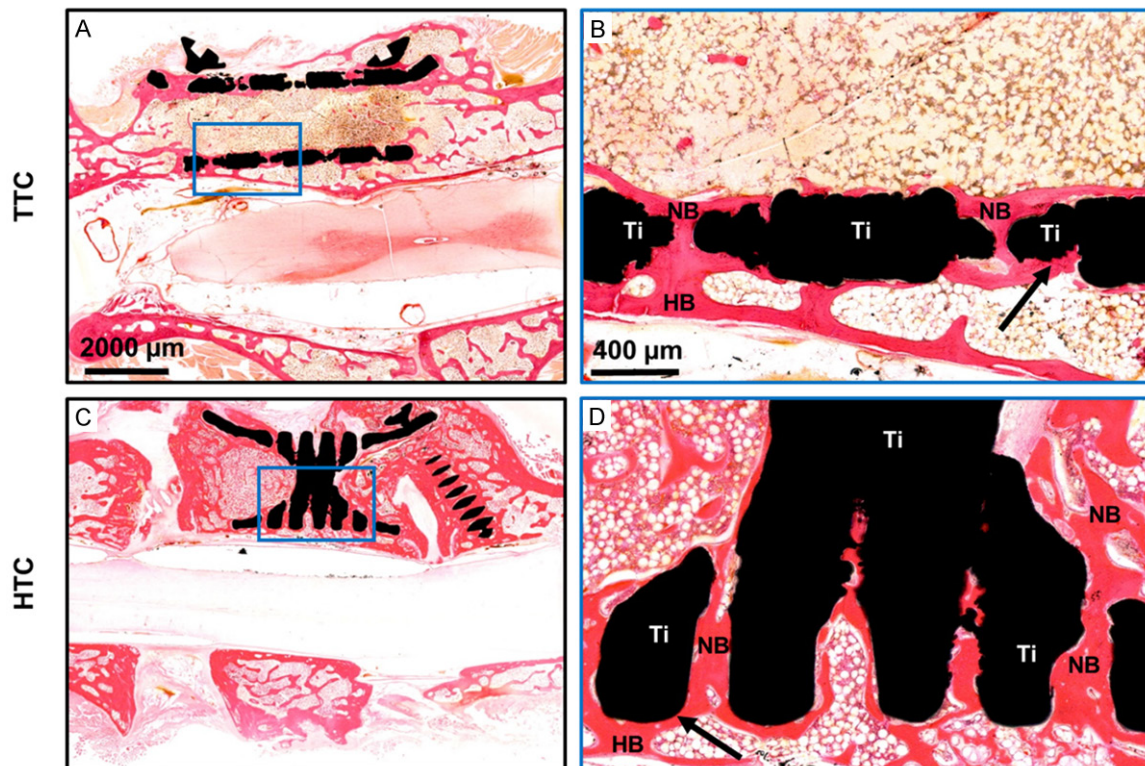


Figure 5. Micro-computed tomography (micro-CT) analysis. A. Analysis of the bone volume fraction (BV/TV) 16 weeks after implantation revealed significantly more bone formation in the helical-shaped titanium cage (HTC) group compared to the traditional titanium cage (TTC) group. B. Two-dimensional micro-CT images of the TTC and HTC 16 weeks after implantation. C. Three-dimensional (3D) micro-CT reconstructed images of the TTC and HTC, where the cage is in red and the bone is grayish-white. All data are expressed as the mean \pm standard deviation (SD). ** $P < 0.01$.



3D-printed titanium cage for cervical vertebral defect repair

Figure 6. Hematoxylin and eosin (H & E) stained histological sections of the traditional titanium cage (TTC) and helical-shaped titanium cage (HTC)-implanted rabbit cervical vertebral defects at 16 weeks. A. TTC-implanted stained tissue sections at lower magnification. B. Higher magnified area of tissue section of TTC shows the integration between the implant and host bone. C. HTC-implanted histological tissue section at lower magnification. D. HTC-implanted tissue section at higher magnification shows bone ingrowth in HTC and excellent osseointegration in the defect. The formation of new bone (in pink) was greater in the HTC group. The black arrows indicate the contact between the implant and host bone. Ti, cage material; NB, new bone; HB, host bone.

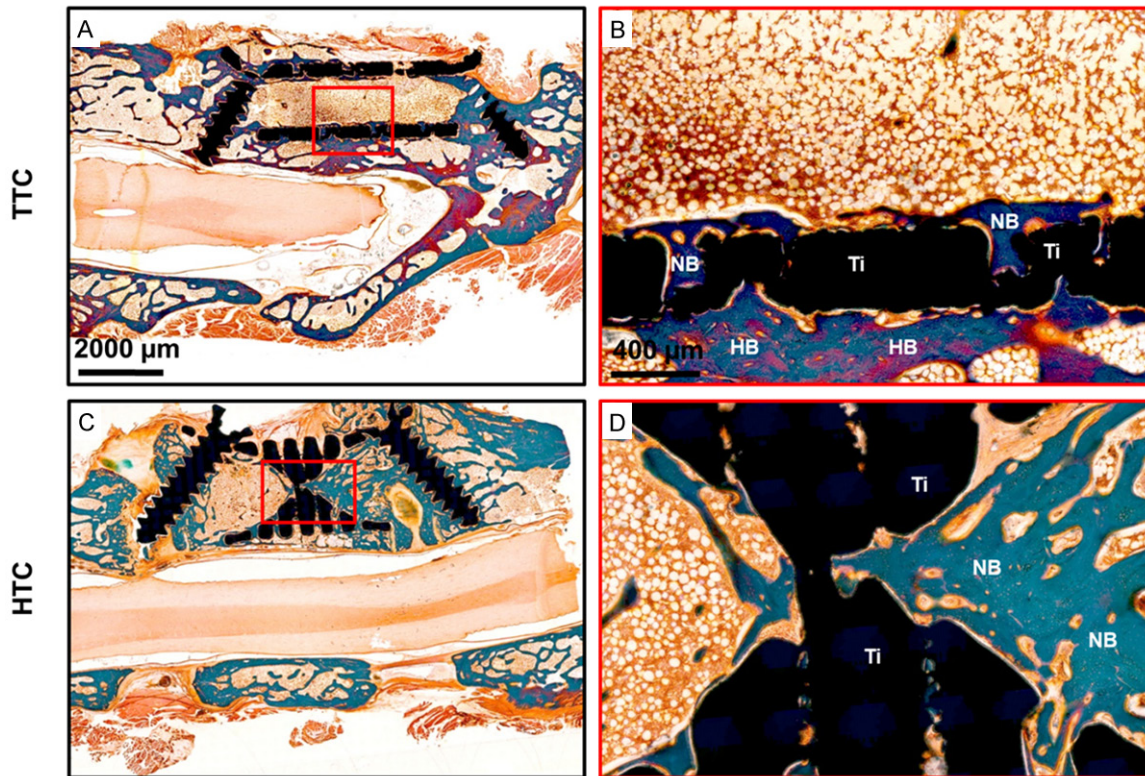


Figure 7. Goldner's trichrome staining of the traditional titanium cage (TTC) and helical-shaped titanium cage (HTC) 16 weeks after implantation in the cervical vertebral defects. A. Stained tissue section with TTC at lower magnification. B. TTC at higher magnification shows bone formation in the TTC. C. HTC-implanted stained tissue section at lower magnification. D. HTC-implanted tissue section at higher magnification. Increased bone ingrowth and more mineralized bone were observed in the HTC compared to TTC. Ti, cage material; NB, new bone; HB, host bone.

vertebral defect model after corpectomy in rabbits. We performed corpectomy and induced vertebral defects in the cervical spine in NZW rabbits, and then implanted the TTC and HTC in the defects. We investigated the *in vivo* biocompatibility, implanted vertebral segment height, osseointegration, and bone ingrowth in the TTC and HTC groups at 16 weeks after implantation.

Cage subsidence is the most common complication after spinal surgery with Ti cages, and can lead to height loss in the surgical segment. The cage design and shape may affect cage subsidence and fusion after cervical fusion sur-

gery [36]. In this study, we measured the operated vertebral segment height after TTC and HTC implantation in a cervical corpectomy model as a predictor of cage subsidence risk. However, many clinical studies have used Ti cages with different designs and shapes for better cervical fusion and evaluation of cage subsidence. One study used a flanged TMC for reconstruction of the CSM and achieved a favorable fusion outcome, although cage subsidence occurred at a rate of 34% [8]. In another study, a box-shaped Ti cage was implanted for anterior cervical fusion, but cage subsidence occurred in a significant number of patients [37]. A dome-shaped cage was evalu-

3D-printed titanium cage for cervical vertebral defect repair

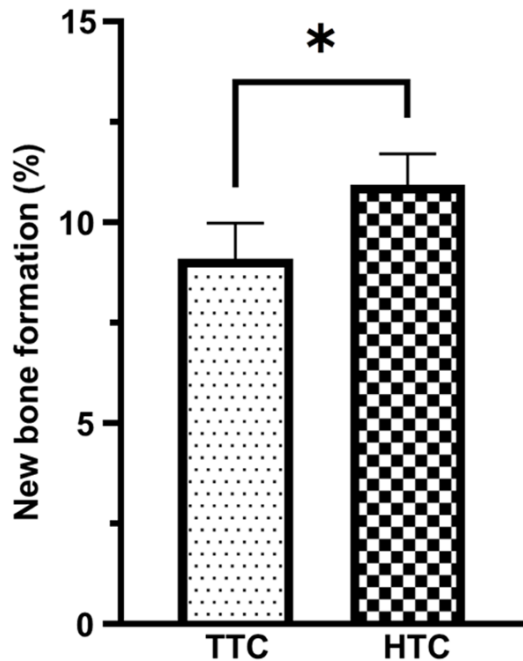


Figure 8. Histomorphometric analysis of the traditional titanium cage (TTC) and helical-shaped titanium cage (HTC) in the cervical vertebral defects. Significant new bone formation was associated with the HTC group 16 weeks after implantation, compared to the TTC group. * $P < 0.05$.

ated in a cervical corpectomy model, and exhibited anti-subsidence capacity [14]. In addition, wing-shaped Ti cages were implanted in patients undergoing cervical fusion in one study, and cage subsidence was evaluated [38]. Expandable Ti cages have also been used, but significant cage subsidence was reported [39]. Our result showed that the TTC implanted vertebral segment height was significantly reduced compared to the HTC, indicating that the TTC was more likely to be susceptible to cage subsidence (Figure 4B). The HTC enabled smooth body motion and had a good porous structure, which might result in lower rates of cage subsidence.

Bone ingrowth into cervical cages is inevitable after corpectomy to evaluate bone fusion efficacy [40]. Moreover, proper osseointegration of Ti implants with host bone is necessary for successful healing of bone defects after implantation [33]. A significant difference in bone ingrowth was confirmed between the TTC and HTC in this study, by H & E and Goldner's trichrome staining (Figures 6 and 7). The HTC resulted in significant new bone formation,

which was assumed to provide faster bone fusion after cervical corpectomy (Figure 8). In addition, excellent osseointegration around the HTC enhanced host bone-implant contact, so the inner structure of the HTC provided a larger surface area for new bone formation. However, the TTC was hollow inside, so bone apposition was low due to the poor surface area of the TTC. Our study suggested that the HTC could be effective for bone defect healing and bone fusion studies.

This study had some limitations: It investigated cage subsidence using a rabbit corpectomy model, which was not sufficient for determining its clinical impact. Therefore, cage subsidence studies using TTC and HTC should be validated in large animal models.

In conclusion, we established a rabbit cervical corpectomy defect and implantation model. The HTC group showed enhanced osseointegration and osteogenesis compared to the TTC group. This preclinical study confirmed the effectiveness of the HTC as a cervical cage, but further studies are required before clinical trials can begin.

Acknowledgements

This work was supported by the Soonchunhyang University Research Fund and by a grant (No. 2015R1A6A1A03032522) of the Basic Science Research Program through the National Research Foundation (NRF) funded by the Ministry of Education, Republic of Korea.

Disclosure of conflict of interest

None.

Address correspondence to: Soobin Im, Department of Neurosurgery, College of Medicine, Soonchunhyang University, Bucheon Hospital, 170 Jomaruro, Womni-gu, Bucheon-si, Gyeonggi-do, South Korea. Tel: +82-32-621-5290; Fax: +82-32-621-5016; E-mail: isbrzw@schmc.ac.kr

References

- [1] Qin R, Chen X, Zhou P, Li M, Hao J and Zhang F. Anterior cervical corpectomy and fusion versus posterior laminoplasty for the treatment of oppressive myelopathy owing to cervical ossification of posterior longitudinal ligament: a meta-analysis. *Eur Spine J* 2018; 27: 1375-1387.

3D-printed titanium cage for cervical vertebral defect repair

- [2] Wen Z, Lu T, Wang Y, Liang H, Gao Z and He X. Anterior cervical corpectomy and fusion and anterior cervical discectomy and fusion using titanium mesh cages for treatment of degenerative cervical pathologies: a literature review. *Med Sci Monit* 2018; 24: 6398-6404.
- [3] Geck MJ and Eismont FJ. Surgical options for the treatment of cervical spondylotic myelopathy. *Orthop Clin North Am* 2002; 33: 329-348.
- [4] Heneghan HM and McCabe JP. Use of autologous bone graft in anterior cervical decompression: morbidity & quality of life analysis. *BMC Musculoskelet Disord* 2009; 10: 158.
- [5] Zeng J, Duan Y, Yang Y, Wang B, Hong Y, Lou J, Ning N and Liu H. Anterior corpectomy and reconstruction using dynamic cervical plate and titanium mesh cage for cervical spondylotic myelopathy: a minimum 5-year follow-up study. *Medicine (Baltimore)* 2018; 97: e9724.
- [6] Chagas H, Domingues F, Aversa A, Vidal Fonseca AL and de Souza JM. Cervical spondylotic myelopathy: 10 years of prospective outcome analysis of anterior decompression and fusion. *Surg Neurol* 2005; Suppl 1: S1:30-35; discussion S31:35-36.
- [7] Chun HJ, Oh SH, Yi HJ and Ko Y. Efficacy and durability of the titanium mesh cage spacer combined with transarticular screw fixation for atlantoaxial instability in rheumatoid arthritis patients. *Spine (Phila Pa 1976)* 2009; 34: 2384-2388.
- [8] Kang JH, Im SB, Yang SM, Chung M, Jeong JH, Kim BT, Hwang SC, Shin DS and Park JH. Surgical reconstruction using a flanged mesh cage without plating for cervical spondylotic myelopathy and a symptomatic ossified posterior longitudinal ligament. *J Korean Neurosurg Soc* 2019; 62: 671-680.
- [9] Sevki K, Mehmet T, Ufuk T, Azmi H, Mercan S and Erkal B. Results of surgical treatment for degenerative cervical myelopathy: anterior cervical corpectomy and stabilization. *Spine (Phila Pa 1976)* 2004; 29: 2493-2500.
- [10] Chen Y, Chen D, Guo Y, Wang X, Lu X, He Z and Yuan W. Subsidence of titanium mesh cage: a study based on 300 cases. *J Spinal Disord Tech* 2008; 21: 489-492.
- [11] Wu J, Luo D, Ye X, Luo X, Yan L and Qian H. Anatomy-related risk factors for the subsidence of titanium mesh cage in cervical reconstruction after one-level corpectomy. *Int J Clin Exp Med* 2015; 8: 7405-7411.
- [12] Jang JW, Lee JK, Lee JH, Hur H, Kim TW and Kim SH. Effect of posterior subsidence on cervical alignment after anterior cervical corpectomy and reconstruction using titanium mesh cages in degenerative cervical disease. *J Clin Neurosci* 2014; 21: 1779-1785.
- [13] Wang Y, Zhan Y, Yang H, Guo H, Zhang H, Zhao Q, Hao D and Wang B. A novel anatomic titanium mesh cage for reducing the subsidence rate after anterior cervical corpectomy: a finite element study. *Sci Rep* 2021; 11: 15399.
- [14] Wang Y, Lu T, He X, Wen Z, Gao Z, Gao Z and Liang H. Effect of dome-shaped titanium mesh cages on cervical endplate under cyclic loading: an in vitro biomechanics study. *Med Sci Monit* 2019; 25: 142-149.
- [15] McGilvray KC, Easley J, Seim HB, Regan D, Berven SH, Hsu WK, Mroz TE and Puttlitz CM. Bony ingrowth potential of 3D-printed porous titanium alloy: a direct comparison of interbody cage materials in an in vivo ovine lumbar fusion model. *Spine J* 2018; 18: 1250-1260.
- [16] Popov VV Jr, Muller-Kamskii G, Kovalevsky A, Dzhenzhera G, Strokin E, Kolomiets A and Ramon J. Design and 3D-printing of titanium bone implants: brief review of approach and clinical cases. *Biomed Eng Lett* 2018; 8: 337-344.
- [17] Zhang W, Sun C, Zhu J, Zhang W, Leng H and Song C. 3D printed porous titanium cages filled with simvastatin hydrogel promotes bone ingrowth and spinal fusion in rhesus macaques. *Biomater Sci* 2020; 8: 4147-4156.
- [18] Choy WJ and Mobbs RJ. Current state of 3D-printed custom-made spinal implants. *Lancet Digit Health* 2019; 1: e149-e150.
- [19] Li P, Jiang W, Yan J, Hu K, Han Z, Wang B, Zhao Y, Cui G, Wang Z, Mao K, Wang Y and Cui F. A novel 3D printed cage with microporous structure and in vivo fusion function. *J Biomed Mater Res A* 2019; 107: 1386-1392.
- [20] Sheha ED, Gandhi SD and Colman MW. 3D printing in spine surgery. *Ann Transl Med* 2019; 7: S164.
- [21] Siu TL, Rogers JM, Lin K, Thompson R and Owbridge M. Custom-made titanium 3-dimensional printed interbody cages for treatment of osteoporotic fracture-related spinal deformity. *World Neurosurg* 2018; 111: 1-5.
- [22] Mangano F, Chambrone L, van Noort R, Miller C, Hatton P and Mangano C. Direct metal laser sintering titanium dental implants: a review of the current literature. *Int J Biomater* 2014; 2014: 461534.
- [23] Żebrowski R, Walczak M, Korga A, Iwan M and Szala M. Effect of shot peening on the mechanical properties and cytotoxicity behaviour of titanium implants produced by 3d printing technology. *J Healthc Eng* 2019; 2019: 8169538.
- [24] Smith GW and Robinson RA. The treatment of certain cervical-spine disorders by anterior removal of the intervertebral disc and interbody fusion. *J Bone Joint Surg Am* 1958; 40: 607-624.

3D-printed titanium cage for cervical vertebral defect repair

- [25] Coelho PG and Jimbo R. Osseointegration of metallic devices: current trends based on implant hardware design. *Arch Biochem Biophys* 2014; 561: 99-108.
- [26] Gehrke SA, Eliers Treichel TL, Pérez-Díaz L, Calvo-Guirado JL, Aramburú Júnior J, Mazón P and de Aza PN. Impact of different titanium implant thread designs on bone healing: a biomechanical and histometric study with an animal model. *J Clin Med* 2019; 8: 777.
- [27] Orsini E, Giavaresi G, Trirè A, Ottani V and Salgarello S. Dental implant thread pitch and its influence on the osseointegration process: an in vivo comparison study. *Int J Oral Maxillofac Implants* 2012; 27: 383-392.
- [28] Chang YS, Oka M, Kobayashi M, Gu HO, Li ZL, Nakamura T and Ikada Y. Significance of interstitial bone ingrowth under load-bearing conditions: a comparison between solid and porous implant materials. *Biomaterials* 1996; 17: 1141-1148.
- [29] Wilke HJ, Kettler A, Goetz C and Claes L. Subsidence resulting from simulated postoperative neck movements: an in vitro investigation with a new cervical fusion cage. *Spine (Phila Pa 1976)* 2000; 25: 2762-2770.
- [30] Shah FA, Trobos M, Thomsen P and Palmquist A. Commercially pure titanium (cp-Ti) versus titanium alloy (Ti6Al4V) materials as bone anchored implants-Is one truly better than the other? *Mater Sci Eng C Mater Biol Appl* 2016; 62: 960-966.
- [31] Agarwal R and García AJ. Biomaterial strategies for engineering implants for enhanced osseointegration and bone repair. *Adv Drug Deliv Rev* 2015; 94: 53-62.
- [32] Gehrke SA, Dedavid BA, Aramburú JSJ, Pérez-Díaz L, Calvo Guirado JL, Canales PM and De Aza PN. Effect of different morphology of titanium surface on the bone healing in defects filled only with blood clot: a new animal study design. *Biomed Res Int* 2018; 2018: 4265474.
- [33] Gittens RA, McLachlan T, Olivares-Navarrete R, Cai Y, Berner S, Tannenbaum R, Schwartz Z, Sandhage KH and Boyan BD. The effects of combined micron-/submicron-scale surface roughness and nanoscale features on cell proliferation and differentiation. *Biomaterials* 2011; 32: 3395-3403.
- [34] Deng F, Liu L, Li Z and Liu J. 3D printed Ti6Al4V bone scaffolds with different pore structure effects on bone ingrowth. *J Biol Eng* 2021; 15: 4.
- [35] Wang H, Su K, Su L, Liang P, Ji P and Wang C. The effect of 3D-printed Ti(6)Al(4)V scaffolds with various macropore structures on osteointegration and osteogenesis: a biomechanical evaluation. *J Mech Behav Biomed Mater* 2018; 88: 488-496.
- [36] Tsai PI, Hsu CC, Chen SY, Wu TH and Huang CC. Biomechanical investigation into the structural design of porous additive manufactured cages using numerical and experimental approaches. *Comput Biol Med* 2016; 76: 14-23.
- [37] Barsa P and Suchomel P. Factors affecting sagittal malalignment due to cage subsidence in standalone cage assisted anterior cervical fusion. *Eur Spine J* 2007; 16: 1395-1400.
- [38] Schmieder K, Wolzik-Grossmann M, Pechlivanis I, Engelhardt M, Scholz M and Harders A. Subsidence of the wing titanium cage after anterior cervical interbody fusion: 2-year follow-up study. *J Neurosurg Spine* 2006; 4: 447-453.
- [39] Weber MH, Fortin M, Shen J, Tay B, Hu SS, Berven S, Burch S, Chou D, Ames C and Deviren V. Graft subsidence and revision rates following anterior cervical corpectomy: a clinical study comparing different interbody cages. *Clin Spine Surg* 2017; 30: E1239-E1245.
- [40] Walsh WR, Pelletier MH, Bertollo N, Christou C and Tan C. Does PEEK/HA enhance bone formation compared with PEEK in a sheep cervical fusion model? *Clin Orthop Relat Res* 2016; 474: 2364-2372.